

## An analytical-numerical procedure for cracking and time-dependent effects in continuous composite beams under service load

Sandeep Chaudhary<sup>†</sup>, Umesh Pendharkar<sup>‡</sup> and A.K. Nagpal<sup>‡</sup>

*Department of Civil Engineering, Indian Institute of Technology, Delhi, Hauz Khas, New Delhi 110016, India*

*(Received May 9, 2005, Accepted April 26 2007)*

**Abstract.** An analytical-numerical procedure has been presented in this paper to take into account the non-linear effects of concrete cracking and time-dependent effects of creep and shrinkage in the concrete portion of the continuous composite beams under service load. The procedure is analytical at the element level and numerical at the structural level. The cracked span length beam element consisting of uncracked zone in middle and cracked zones near the ends has been proposed to reduce the computational effort. The progressive nature of cracking of concrete has been taken into account by division of the time into a number of time intervals. Closed form expressions for stiffness matrix, load vector, crack lengths and mid-span deflection of the beam element have been presented in order to reduce the computational effort and book-keeping. The procedure has been validated by comparison with the experimental and analytical results reported elsewhere and with FEM. The procedure can be readily extended for the analysis of composite building frames where saving in computational effort would be very considerable.

**Keywords:** creep; shrinkage; cracking; composite beam; closed form expressions.

---

### 1. Introduction

The composite beam (Fig. 1) is one of the economical forms of construction. Combination of steel and concrete systems has been conceived on the premises that each type of construction offers a natural advantage which when utilized together results in an efficient system. In continuous composite beams, the time-dependent effects of creep and shrinkage in concrete can lead to the progressive cracking of concrete slab near interior supports and result in considerable moment redistribution along with increase in deflections.

Extensive literature is available on time-dependent analysis of continuous composite beams up to ultimate load stage. Such procedures have been presented by Sakr and Lapos 1998, Kwak and Seo (2000, 2002a, 2002b), Mari *et al.* (2003) and Fragiaco *et al.* (2004). The procedures take into account the progressive cracking. In these procedures, the division of the beam along the length and across the section is required to take into account the non-linear behaviour under ultimate load but this division leads to considerable increase in the computational effort.

---

<sup>†</sup>Research Scholar

<sup>‡</sup>Professor, Corresponding Author, E-mail: [aknagpal@civil.iitd.ernet.in](mailto:aknagpal@civil.iitd.ernet.in)

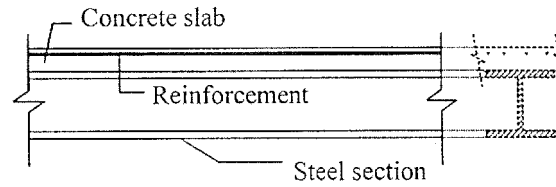


Fig. 1 Composite beam

Some numerical procedures have been proposed for the time-dependent analysis of continuous composite beams under service load. A coupled system of equations has been proposed by Dezi and Tarantino (1993a, 1993b) for inelastic analysis of continuous composite beams by discretising the time into a number of time intervals. The beam has been considered to be uncracked and is discretised along its axis. Subsequently, the time-dependent analysis of prestressed continuous composite beams has also been proposed using the coupled system of equations (Dezi *et al.* 1995). Cracking is neglected in this method as it is assumed that prestressing is sufficient to prevent cracking. A simplification in the method has been proposed later on to carry out the analysis in a single time step (Dezi *et al.* 1996). A simplified numerical model using the closed form expressions has been presented to evaluate the creep and shrinkage effects in composite beams (Amadio and Fragiaco 1997) neglecting the cracking.

A simple analytical procedure for the time-dependent analysis of two equal span continuous composite beams under service load, taking into account cracking, has been proposed by Gilbert and Bradford (1995). The transformed section approach has been used and the beam is taken as one element without subdivision along the length and across the cross-section. The analysis is carried out in single time step and the same crack lengths are assumed for the entire time interval beginning from the time of application of the load. The progressive nature of cracking i.e., continuous change in crack length of the beam with time is therefore not taken into account in this approach. Tension stiffening has also been neglected in the procedure. This analytical procedure has been further extended by Bradford *et al.* (2002) making it applicable for two unequal span continuous composite beams. The procedure though convenient for two-span beams, would tend to become tedious if extended to beams having more than two spans.

On the other hand application of a purely numerical approach (Sakr and Lapos 1998, Kwak and Seo 2000, 2002a, 2002b, Mari *et al.* 2003 and Fragiaco *et al.* 2004) for analysis at service load in which the subdivision along the length and cross-section is carried out would require a too large computational effort and elaborate book keeping in order to determine the crack lengths, stresses etc.

Therefore, for service load, an analytical-numerical procedure has been presented in this paper to take into account the non-linear effects of concrete cracking and time-dependent effects of creep and shrinkage in continuous composite beams. The procedure is analytical at the element level and numerical at the structural level. The cracked span length beam element consisting of uncracked zone in the middle and cracked zones near the ends has been proposed. Closed form expressions for stiffness matrix, load vector, crack lengths and mid-span deflection of the beam element have been presented. This approach reduces considerably the computational effort. The proposed procedure takes into account the progressive nature of cracking of concrete by division of the time into a number of time intervals. The tension stiffening effect has also been incorporated in the proposed procedure. The procedure has been validated by comparison with the experimental results (Gilbert and Bradford 1992), analytical results (Gilbert and Bradford 1995) and with finite element method. The procedure can be readily extended for analysis of composite building frames where saving in computational effort would be very considerable.

### 2. Cross-section analysis

A typical composite cross-section along with the strain distribution is shown in Fig. 2. It is assumed that a plane cross-section remains plane. Slip between the slab and steel section has been neglected since the earlier experiments and studies (Bradford and Gilbert 1991 and 1992) have shown that the slip under sustained service load can be neglected provided the shear connectors are at a sufficient close spacing. The closer spacing is desirable from design considerations also, since this reduces the deflections. Under service load, the stress- strain relationship of concrete, prior to cracking, is assumed to be linearly elastic in both compression and tension. The concrete portion across the cross-section is assumed to be completely cracked, when the top fiber stress of the concrete slab exceeds the tensile strength of concrete,  $f_t$ , since the moment required for cracking the slab fully is only slightly larger than the moment required for cracking the top fiber only (Bradford *et al.* 2002). The stress-strain relationship for steel in both tension and compression is also assumed to be linear and stresses in steel section are assumed to be below the yield stress, this would generally be the case when high strength steel sections are used. Further, it is assumed that the construction is propped. Since neutral axis varies with time and is also different for the cracked and the uncracked cross-sections, the top fiber of cross-section has been selected as the reference axis.

The instantaneous curvature,  $\rho^{it}$ , the instantaneous top fiber strain,  $\epsilon^{it}$  and the instantaneous top fiber stress,  $\sigma^{it}$  due to an applied moment  $N^{it}$  (the superscript, *it*, in quantities, here and subsequently, in other quantities indicates the instantaneous value of the quantity), at a cross-section (Fig. 2) are given as (Gilbert 1988).

$$\rho^{it} = \frac{AM^{it}}{E_c(AI - B^2)}; \quad \epsilon^{it} = \frac{BM^{it}}{E_c(AI - B^2)}; \quad \sigma^{it} = E_c \epsilon^{it} \tag{1-3}$$

where  $E_c$ = modulus of elasticity of concrete;  $A$  = area of the transformed cross-section and  $B, I$  = first and second moment of area of the transformed cross-section about the reference axis (top fibre). It may be noted that when the concrete portion across the cross-section is completely cracked, the properties of the cross-section are those of the transformed steel section and reinforcement only with  $B$  and  $I$  being evaluated about the top fibre of the composite cross-section.

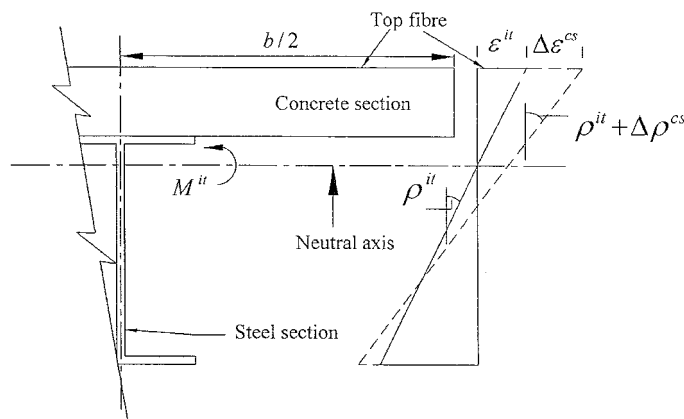


Fig. 2 Strain distribution across the cross-section

In an intermediate span of a continuous composite beam, there may be two cracked zones near the ends and an uncracked zone in the middle.

First consider a cross-section in the uncracked zone. Let the instantaneous curvature, the instantaneous top fiber strain, and the instantaneous top fiber stress be designated as  $\rho_{un}^{it}$ ,  $\varepsilon_{un}^{it}$ ,  $\sigma_{un}^{it}$  respectively where the subscript, *un* in quantities here and subsequently in other quantities indicates that the quantities are evaluated using uncracked cross-sectional properties. Accordingly,  $\rho_{un}^{it}$ ,  $\varepsilon_{un}^{it}$ ,  $\sigma_{un}^{it}$  are evaluated from Eqs. (1)-(3) respectively on using uncracked cross-sectional properties.

Consider now, the effect of creep and shrinkage in this cross-section. Assuming the concrete to be completely unrestrained, in a time interval beginning from the time of application of load, the change in curvature and the top fiber strain would be  $\Delta\phi\rho_{un}^{it}$  and  $\Delta\phi\varepsilon_{un}^{it} + \Delta\varepsilon^{sh}$  respectively where  $\Delta\phi$ ,  $\Delta\varepsilon^{sh}$  = creep coefficient and shrinkage strain respectively at the end of the time interval. To restrain these changes, gradually applied axial force  $-\Delta N$  and the bending moment  $-\Delta M$  are required which are given as (Gilbert 1988).

$$\Delta N = \bar{E}_e[\Delta\phi(A_c\varepsilon_{un}^{it} - B_c\rho_{un}^{it}) + \Delta\varepsilon^{sh}A_c]; \quad \Delta M = \bar{E}_e[\Delta\phi(-B_c\varepsilon_{un}^{it} + I_c\rho_{un}^{it}) - \Delta\varepsilon^{sh}B_c] \quad (4,5)$$

where  $A_c$  = area of concrete;  $B_c$ ,  $I_c$  = first moment of area and second moment of area of concrete about the top fiber and  $\bar{E}_e$  = age-adjusted effective modulus of concrete given as  $E_c/(1+\chi\Delta\phi)$  in which  $\chi$  = aging coefficient. It may be noted that the value of  $\chi$  is different for creep and shrinkage (Amadio and Fragiaco 1997). However, the use of two values of  $\chi$  will lead to complex equations, therefore the same value of  $\chi$  is considered for creep and shrinkage. The error on this account is likely to be small.

Equilibrium is restored by applying  $\Delta N$  and  $\Delta M$  on the cross-section. The change in curvature of the cross-section,  $\Delta\rho_{un}^{cs}$  and the change in the top fiber strain of the cross-section,  $\Delta\varepsilon_{un}^{cs}$  due to  $\Delta N$  and  $\Delta M$  are given as

$$\Delta\rho_{un}^{cs} = \frac{\bar{A}_e\Delta M + \bar{B}_e\Delta N}{\bar{E}_e(\bar{A}_e\bar{I}_e - \bar{B}_e^2)}, \quad \Delta\varepsilon_{un}^{cs} = \frac{\bar{B}_e\Delta M + \bar{I}_e\Delta N}{\bar{E}_e(\bar{A}_e\bar{I}_e - \bar{B}_e^2)} \quad (6,7)$$

where the superscript, *cs* in the quantities,  $\Delta\rho$ ,  $\Delta\varepsilon$  and subsequently in other quantities indicates that the quantities arise from both creep and shrinkage and  $\bar{A}_e$ ,  $\bar{B}_e$ ,  $\bar{I}_e$  = age-adjusted transformed area, first moment of area and second moment of area of the uncracked cross-section about the reference axis and are evaluated using the modular ratio  $E_s/\bar{E}_e$ .

By rearranging Eq. (6),  $\Delta\rho_{un}^{cs}$  can be expressed as a sum of two terms (Gilbert and Bradford 1995): (1) the change in curvature due to creep,  $\Delta\varepsilon_{un}^c\rho_{un}^{it}$  and (2) the change in curvature due to shrinkage,  $\Delta\rho_{un}^s$ . The quantities  $\Delta\beta_{un}^c$  and  $\Delta\rho_{un}^s$  are given as

$$\Delta\beta_{un}^c = \frac{\Delta\phi(A_cB\bar{B}_e - B_cB\bar{A}_e - B_cA\bar{B}_e + I_cA\bar{A}_e)}{A(\bar{A}_e\bar{I}_e - \bar{B}_e^2)}; \quad \Delta\rho_{un}^s = \Delta\varepsilon^{sh}\frac{(\bar{B}_eA_c - \bar{A}_eB_c)}{(\bar{A}_e\bar{I}_e - \bar{B}_e^2)} \quad (8,9)$$

where the superscripts *c*, *s* in the quantities  $\Delta\beta$ ,  $\Delta\rho$  and subsequently in other quantities indicate that these quantities arise from creep and shrinkage respectively.

Similarly, by rearranging Eq. (7),  $\Delta\varepsilon_{un}^{cs}$  can be expressed as a sum of two terms: (1) change in the top fiber strain due to creep,  $\Delta\lambda_{un}^c\varepsilon_{un}^{it}$  and (2) change in the top fiber strain due to shrinkage,  $\Delta\varepsilon_{un}^s$ . The quantities  $\Delta\lambda_{un}^c$  and  $\Delta\varepsilon_{un}^s$  are given as

$$\Delta\lambda_{un}^c = \frac{\Delta\phi(A_c B \bar{I}_e - B_c B \bar{B}_e - B_c A \bar{I}_e + I_c A \bar{B}_e)}{B(\bar{A}_e \bar{I}_e - \bar{B}_e^2)}; \quad \Delta\varepsilon_{un}^s = \Delta\varepsilon^{sh} \frac{(\bar{I}_e A_c - \bar{B}_e B_c)}{(\bar{A}_e \bar{I}_e - \bar{B}_e^2)} \quad (10,11)$$

In indeterminate structures, an additional moment  $\Delta M^{id}$  (the superscript, *id*, here and subsequently, in other quantities indicates that the quantity arises in indeterminate structures due to redistribution of forces caused by creep and shrinkage) is generated gradually. The additional curvature,  $\Delta\rho_{un}^{id}$ , the additional top fiber strain,  $\Delta\varepsilon_{un}^{id}$  and the additional top fiber stress,  $\Delta\sigma_{un}^{id}$  due to  $\Delta M^{id}$  are given by Eqs. (1) - (3) respectively on replacement of  $M^t$  by  $\Delta M^{id}$ ,  $E_e$  by  $\bar{E}_e$  and  $A, B, I$  by  $\bar{A}_e, \bar{B}_e, \bar{I}_e$  of the uncracked cross-section.

The total curvature,  $\rho_{un}^t$ , the total top fiber strain,  $\varepsilon_{un}^t$  and the total top fiber stress,  $\sigma_{un}^t$  (the superscript, *t* in the quantities here and subsequently in other quantities, indicates the total value of quantity at the end of a time interval) of an uncracked cross-section at the end of the time interval are obtained by adding the changes in the quantities in the time interval to their instantaneous values respectively, as

$$\rho_{un}^t = \rho_{un}^{it} + \Delta\rho_{un}^{cs} + \Delta\rho_{un}^{id}; \quad (12)$$

$$\varepsilon_{un}^t = \varepsilon_{un}^{it} + \Delta\varepsilon_{un}^{cs} + \Delta\varepsilon_{un}^{id}; \quad (13)$$

$$\sigma_{un}^t = \sigma_{un}^t + \bar{E}_e[\Delta\varepsilon_{un}^{cs} - \Delta\phi\varepsilon_{un} - \Delta\varepsilon^{sh}] + \Delta\sigma_{un}^{id} \quad (14)$$

Next consider a cross-section in the cracked zone. The tension stiffening effect is taken into account by considering the cross-section in two states, uncracked and cracked. The cracked cross-section in the uncracked state has the same properties as that of the uncracked cross-section. In the cracked state, as stated earlier, the properties of the cross-section are those of the transformed steel section and reinforcement only.

The instantaneous curvature  $\rho_{ts}^{it}$  and instantaneous strain in the top fiber  $\varepsilon_{ts}^{it}$  (the subscript, *ts* here and subsequently in other quantities indicates that the tension stiffening effect has been taken into account) of the cross-section are equal to  $\eta\rho_{un}^{it} + \xi\rho_{cr}^{it}$  and  $\eta\varepsilon_{un}^{it} + \xi\varepsilon_{cr}^{it}$  respectively (the subscript, *cr* here and subsequently in other quantities indicates the cracked state of the cross-section) where  $\xi$  = interpolation coefficient and  $\eta = 1 - \xi$ .  $\rho_{cr}^{it}, \varepsilon_{cr}^{it}$  are evaluated from Eqs. (1) and (2) respectively on using the cracked state properties of the cross-section.

The interpolation coefficient,  $\xi$  is evaluated by the following expression, with a minor modification based on study by Albrecht *et al.* (2003) to the expression proposed by CEB-FIP Model Code (1990), as

$$\xi = 1 - \kappa(f_t / \sigma_{un})^2 \quad (15)$$

where  $\kappa = a$  factor for reduction in interpolation coefficient with time and  $\sigma_{un}$  = the tensile stress in the reference axis to be evaluated from Eq. (3) assuming the cross-section to be in the uncracked state.

Based on a study by Albrecht *et al.* (2003), the value of  $\kappa$  has been assumed to be 1.0 for the instantaneous analysis and  $0.65 - 0.15(\Delta\phi / \phi_u)$  at any time instant for time-dependent analysis where  $\phi_u$  = the ultimate creep coefficient.

Consider now, the effect of creep and shrinkage in a cross-section in the cracked zone. In the uncracked state, the change in curvature and strain is evaluated in the same manner as explained earlier for the uncracked zone (Eqs. (6)-(11)). In the cracked state, no change in curvature and strain takes place owing to

creep and shrinkage. However, the changes occur in both the cracked and uncracked states owing to additional moment,  $\Delta M^{id}$  (in indeterminate structures). For the cracked state, the additional curvature,  $\Delta \rho_{cr}^{id}$  and the additional top fiber strain,  $\Delta \varepsilon_{cr}^{id}$  due to  $\Delta M^{id}$  are given by Eqs. (1) and (2) respectively on replacement of  $M^i$  by  $\Delta M^{id}$  and on using the cracked state properties of the cross-section. The total curvature,  $\rho_{ts}^t$  and the total top fiber strain,  $\varepsilon_{ts}^t$  of a cross-section in the cracked zone, at the end of the time interval are obtained by adding the changes in the uncracked and the cracked state of cross-section to the instantaneous values and are given as

$$\rho_{ts}^t = \xi \rho_{cr}^{it} + \eta \rho_{un}^{it} + \eta \Delta \rho_{un}^{cs} + \xi \Delta \rho_{cr}^{id} + \eta \Delta \rho_{un}^{id}; \quad \varepsilon_{ts}^t = \xi \varepsilon_{cr}^{it} + \eta \varepsilon_{un}^{it} + \eta \Delta \varepsilon_{un}^{cs} + \xi \Delta \varepsilon_{cr}^{id} + \eta \Delta \varepsilon_{un}^{id} \quad (16-17)$$

The total moment,  $M^t$  at the end of a time interval at a cross-section, both in the uncracked and the cracked zone, is expressed as  $M^t = M^{it} = \Delta M^{id}$ .

### 3. Cracked span length beam element

Fig. 3 shows a typical bending moment diagram of a continuous beam due to vertical load. Concrete would crack near interior supports if the tensile stress in the top fiber of a cross-section exceeds the tensile strength of concrete. A typical cracked span length beam element therefore consists of three zones, two cracked zones of length  $x_A, x_B$ , near ends A and B respectively, and an uncracked zone in the middle (Fig. 4).

The stiffness matrix and the load vector of a cracked span length beam element are of interest. In order to evaluate these, releases 1 and 2 are introduced at the ends (Fig. 5).

For the evaluation of stiffness matrix, the flexibility coefficients  $f_{11}, f_{12}, f_{21}, f_{22}$  that are required can be found by the principle of virtual work using  $m_1$  and  $m_2$  diagrams (Fig. 6), as

$$f_{11} = \int_0^L \frac{m_1^2 dx}{E_c I^{na}}; \quad f_{12} = f_{21} = \int_0^L \frac{m_1 m_2 dx}{E_c I^{na}}; \quad f_{22} = \int_0^L \frac{m_2^2 dx}{E_c I^{na}} \quad (18-20)$$

where  $I^{na} [= (AI - B^2)/A]$  = moment of inertia of transformed cross-section in the uncracked or cracked state, about the neutral axis (Fig. 2).

Eqs. (18)-(20) are to be integrated for the uncracked zone and the two cracked zones. For a cross-section in the uncracked zone,  $1/E_c I^{na}$  is replaced by  $1/E_c I_{un}^{na}$  whereas for a cross-section in a cracked

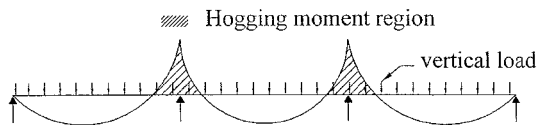


Fig. 3 Typical bending moment diagram of a continuous beam

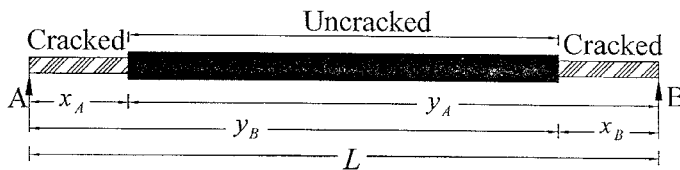


Fig. 4 Zones in a typical cracked span length beam element



Fig. 5 Cracked span length released beam element

zone, considering the tension stiffening effect,  $1/E_c I^{na}$  is to be replaced by  $1/E_c I_{is}^{na} (= \xi/E_c I_{cr}^{na} + \eta/E_c I_{un}^{na})$ .

A single interpolation coefficient has been assumed for each cracked zone. The interpolation coefficient for cracked zones near ends A and B are termed as  $\xi_A, \xi_B$  respectively and are evaluated from Eq. (15) in which  $\sigma_{un}$  is replaced by the representative stresses,  $\sigma_{un,A}, \sigma_{un,B}$  respectively that are obtained by dividing the area of stress diagrams  $\sigma_{un}$  over crack lengths  $x_A, x_B$  respectively by respective crack lengths  $x_A, x_B$ .

The closed form expressions for  $f_{11}, f_{12}, f_{21}, f_{22}$  obtained from Eqs. (18)-(20), incorporating tension stiffening effect, are given in Appendix A. Stiffness matrix  $[k]$  is the inverse of flexibility matrix and the terms of stiffness matrix,  $k_{11}, k_{12}, k_{21}, k_{22}$  may be expressed in the closed form as

$$k_{11} = f_{22}' / (f_{11}f_{22} - f_{21}f_{12}); k_{12} = k_{21} = -f_{12}' / (f_{11}f_{22} - f_{21}f_{12}); k_{22} = f_{11}' / (f_{11}f_{22} - f_{21}f_{12}) \quad (21-23)$$

For evaluation of the fixed end moments, additionally the rotations at the ends are required. The end rotations of the released beam element due to applied load or creep or shrinkage are found by integrating  $m_1$  and  $m_2$  diagrams respectively with the corresponding curvature diagram.

In particular, for the case of uniformly distributed span load,  $w$  (Fig. 7), the instantaneous rotations  $\theta_A^{it}$  and  $\theta_B^{it}$  at the ends A and B respectively, may be expressed in the closed form, on integrating  $m_1$  and  $m_2$  diagrams respectively with the curvature diagram  $\rho^{it}(x)$  which is obtained from Eq. (1) on substitution of  $M^{it}$  by  $wLx/2 - wx^2/2$  where  $x =$  distance of cross-section from an end. The expressions for  $\theta_A^{it}$  and  $\theta_B^{it}$  are obtained as

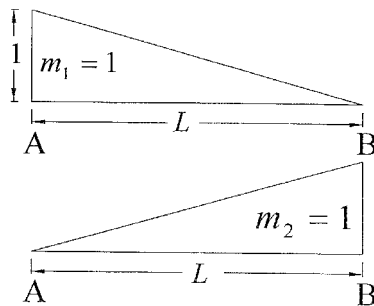


Fig. 6  $m_1$  and  $m_2$  diagrams

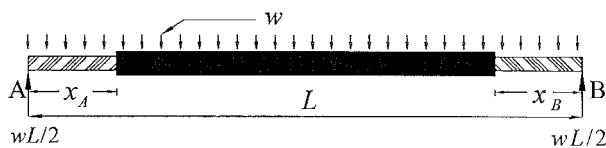


Fig. 7 Beam element subjected to uniformly distributed span load

$$\theta_A^{it} = \frac{w}{24E_c L} \left[ \frac{3\xi_A y_A^4 - 3\xi_B x_B^4 - \eta_A L^4 - 4\xi_A L y_A^3 + 4\xi_B L x_B^3}{I_{un}^{na}} + \frac{3\xi_B x_B^4 - 3\xi_A y_A^4 - \xi_A L^4 - 4\xi_B L x_B^3 + 4\xi_A L y_A^3}{I_{cr}^{na}} \right] \quad (24)$$

$$\theta_B^{it} = \frac{w}{24E_c L} \left[ \frac{3\xi_A x_A^4 - 3\xi_B y_B^4 + \eta_B L^4 + 4\xi_B L y_B^3 - 4\xi_A L x_A^3}{I_{un}^{na}} + \frac{3\xi_B y_B^4 - 3\xi_A x_A^4 + \xi_B L^4 + 4\xi_A L x_A^3 - 4\xi_B L y_B^3}{I_{cr}^{na}} \right] \quad (25)$$

For a beam element, subjected to uniformly distributed span load,  $w$  and also additionally the instantaneous moments  $M_A^{it}$ ,  $M_B^{it}$  at the ends A and B respectively (Fig. 8), the instantaneous rotations  $\theta_A^{it}$ ,  $\theta_B^{it}$  may be expressed in the closed form, on integrating  $m_1$  and  $m_2$  diagrams respectively with  $\rho^{it}(x)$ , which is obtained from Eq. (1) on substitution of  $M^i$  by  $R_B^{it}x + M_B^{it} - wx^2/2$  and  $R_A^{it}x - M_A^{it} - wx^2/2$  respectively where  $R_A^{it}$ ,  $R_B^{it}$  = the instantaneous reactions at the ends A and B respectively and  $x$  = distance of cross-section from end B for  $\theta_A^{it}$  and from end A for  $\theta_B^{it}$ . The expressions for  $\theta_A^{it}$  and  $\theta_B^{it}$  are obtained as

$$\begin{aligned} \theta_A^{it} = & \left[ 1/(24E_c I_{un}^{na} L) \right] \left[ -8R_B^{it}(\eta_A L^3 + \xi_A y_A^3 - \xi_B x_B^3) - 12M_B^{it}(\eta_A L^2 + \xi_A y_A^2 - \xi_B x_B^2) + 3w(\eta_A L^4 + \xi_A y_A^4 - \xi_B x_B^4) \right] \\ & + \left[ 1/(24E_c I_{cr}^{na} L) \right] \left[ -8R_B^{it}(\xi_B x_B^3 + \xi_A L^3 - \xi_A y_A^3) - 12M_B^{it}(\xi_B x_B^2 + \xi_A L^2 - \xi_A y_A^2) + 3w(\xi_B x_B^4 + \xi_A L^4 - \xi_A y_A^4) \right] \end{aligned} \quad (26)$$

$$\begin{aligned} \theta_B^{it} = & \left[ 1/(24E_c I_{un}^{na} L) \right] \left[ 8R_A^{it}(\eta_B L^3 + \xi_B y_B^3 - \xi_A x_A^3) - 12M_A^{it}(\eta_B L^2 + \xi_B y_B^2 - \xi_A x_A^2) - 3w(\eta_B L^4 + \xi_B y_B^4 - \xi_A x_A^4) \right] \\ & + \left[ 1/(24E_c I_{cr}^{na} L) \right] \left[ 8R_A^{it}(\xi_A x_A^3 + \xi_B L^3 - \xi_B y_B^3) - 12M_A^{it}(\xi_A x_A^2 + \xi_B L^2 - \xi_B y_B^2) - 3w(\xi_A x_A^4 + \xi_B L^4 - \xi_B y_B^4) \right] \end{aligned} \quad (27)$$

The first terms in Eqs. (26) and (27) are the contributions of the uncracked zone and the uncracked state of the cracked zone whereas the second terms are the contributions of the cracked state of the cracked zone.

The mid-span deflection,  $d_m$  of a beam element is also of interest and may be expressed as (Elbadry *et al.* 2003):

$$d_m = (1/2) \int_0^{L/2} \rho(x)x dx + (L/2) \int_{L/2}^L \rho(x)(1-x/L) dx \quad (28)$$

For the beam element shown in Fig. 8, instantaneous mid-span deflection  $d_m^{it}$  may be expressed in the closed form, on replacing  $\rho(x)$  by  $\rho^{it}(x)$ , as

$$d_m^{it} = \left[ \xi_A \left( \frac{R_A^{it} x_A^3}{6} - \frac{M_A^{it} x_A^2}{4} - \frac{w x_A^4}{16} \right) + \xi_B \left( \frac{R_B^{it} x_B^3}{6} + \frac{M_B^{it} x_B^2}{4} - \frac{w x_B^4}{16} \right) \right] \left[ \frac{1}{E_c I_{cr}^{na}} - \frac{1}{E_c I_{un}^{na}} \right] + \left[ \frac{M_B^{it} - M_A^{it}}{16} + \frac{5wL^2}{384} \right] \frac{L^2}{E_c I_{un}^{na}} \quad (29)$$

Creep in the concrete increases the curvature of the uncracked zone and the uncracked state of the

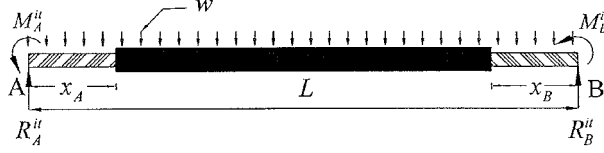


Fig. 8 Beam element subjected to uniformly distributed span load and instantaneous end moments

cracked zone by a factor  $\Delta\beta_{un}^c$  (Eq. (8) ) which leads to the change in end rotations,  $\Delta\theta_A^c, \Delta\theta_B^c$  if the ends are not restrained against the rotation. Since the creep does not take place in the cracked state, the rotations  $\Delta\theta_A^c, \Delta\theta_B^c$  can be expressed from Eqs. (26) and (27) respectively on dropping the second terms involving the cracked state and multiplying the remaining terms by  $\Delta\beta_{un}^c$ , as

$$\Delta\theta_A^c = \left[ \Delta\beta_{un}^c / (24E_c I_{un}^{na} L) \right] \left[ -8R_B^u (\eta_A L^3 + \xi_A y_A^3 - \xi_B x_B^3) - 12M_B^u (\eta_A L^2 + \xi_A y_A^2 - \xi_B x_B^2) + 3w (\eta_A L^4 + \xi_A y_A^4 - \xi_B x_B^4) \right] \quad (30)$$

$$\Delta\theta_B^c = \left[ \Delta\beta_{un}^c / (24E_c I_{un}^{na} L) \right] \left[ 8R_A^u (\eta_B L^3 + \xi_B y_B^3 - \xi_A x_A^3) - 12M_A^u (\eta_B L^2 + \xi_B y_B^2 - \xi_A x_A^2) - 3w (\eta_B L^4 + \xi_B y_B^4 - \xi_A x_A^4) \right] \quad (31)$$

The change in mid-span deflection,  $\Delta d_m^c$ , owing to creep can also be expressed similarly from Eq. (29), as

$$\Delta d_m^c = \Delta\beta_{un}^c \left[ -\xi_A \left( \frac{R_A^u x_A^3}{6} - \frac{M_A^u x_A^2}{4} - \frac{w x_A^4}{16} \right) - \xi_B \left( \frac{R_B^u x_B^3}{6} + \frac{M_B^u x_B^2}{4} - \frac{w x_B^4}{16} \right) + L^2 \left( \frac{M_B^u - M_A^u}{16} + \frac{5wL^2}{384} \right) \right] \frac{1}{E_c I_{un}^{na}} \quad (32)$$

Shrinkage in the concrete causes a constant curvature,  $\Delta\rho_{un}^s$  (Eq. (9) ) in the uncracked zone and in the uncracked state of the cracked zone which leads to the change in end rotations,  $\Delta\theta_A^s, \Delta\theta_B^s$ , if the ends are not restrained against rotations. These rotations may be expressed in the closed form, on integrating  $m_1$  and  $m_2$  diagrams respectively with the curvature diagram,  $\Delta\rho_{un}^s$  for the uncracked zone and  $\eta\Delta\rho_{un}^s$  for the cracked zone, as

$$\Delta\theta_A^s = \left[ \Delta\rho_{un}^s / (2L) \right] \left[ \xi_B x_B^2 - \xi_A y_A^2 - \eta_A L^2 \right]; \quad \Delta\theta_B^s = \left[ \Delta\rho_{un}^s / (2L) \right] \left[ \eta_B L^2 + \xi_B y_B^2 - \xi_A x_A^2 \right] \quad (33,34)$$

Similarly, the change in mid-span deflection due to shrinkage,  $\Delta d_m^s$  may be expressed in the closed form from Eq. (28), on replacing  $\rho(x)$  by  $\Delta\rho_{un}^s$  for the uncracked zone and by  $\eta\Delta\rho_{un}^s$  for the cracked zone, as

$$\Delta d_m^s = (\Delta\rho_{un}^s / 8) (L^2 - 2\xi_A x_A^2 - 2\xi_B x_B^2) \quad (35)$$

The closed form expression for  $\Delta d_m^{id}$ , the additional mid-span deflection due to  $\Delta M^{id}$ , may be obtained from Eq. (29), on dropping the terms related to  $w$ , replacing  $R_A^u, R_B^u, M_A^u, M_B^u$  by  $\Delta R_A^{id}, \Delta R_B^{id}, \Delta M_A^{id}, \Delta M_B^{id}$  (the changes in end reactions and moments resulting from creep and shrinkage) respectively and on replacing  $E_c I_{un}^{na}$  by  $\bar{E}_e \bar{I}_{e,un}^{na}$  (since  $\Delta M^{id}$  is generated gradually), as

$$\Delta d_m^{id} = \left[ \xi_A \left( \frac{\Delta R_A^{id} x_A^3}{6} - \frac{\Delta M_A^{id} x_A^2}{4} \right) + \xi_B \left( \frac{\Delta R_B^{id} x_B^3}{6} + \frac{\Delta M_B^{id} x_B^2}{4} \right) \right] \left[ \frac{1}{E_c I_{e,cr}^{na}} - \frac{1}{\bar{E}_e \bar{I}_{e,un}^{na}} \right] + \frac{L^2 (\Delta M_B^{id} - \Delta M_A^{id})}{16 \bar{E}_e \bar{I}_{e,un}^{na}} \quad (36)$$

where  $\bar{I}_{e,un}^{na}$  = moment of inertia of the uncracked state of a cross-section (having age -adjusted properties) respectively.

The total mid-span deflection,  $d_m^t$  at end of a time interval (beginning from the time of application of load) consists of  $d_m^{it}$ ,  $\Delta d_m^s$ ,  $\Delta d_m^s$  and  $\Delta d_m^{id}$  and may be expressed as

$$d_m^t = d_m^{it} + \Delta d_m^f + \Delta d_m^s + \Delta d_m^{id} \quad (37)$$

#### 4. Analysis of continuous composite beams

The analysis of continuous composite beams is carried out in two parts. In the first part, instantaneous analysis is carried out using an iterative method (Ghali *et al.* 2002) to establish the instantaneous crack lengths. In the second part, time-dependent analysis is carried out by dividing the time into a number of time intervals. The cracked span length beam elements along with the closed form expressions are used in both the parts.

##### 4.1 Instantaneous Analysis

An iterative process is required to establish the instantaneous crack lengths, interpolation coefficients and bending moment at time  $t_1$ , the time of application of load. For a typical iterative cycle, a displacement analysis is carried out for the residual force vector,  $\{E_f(t_1)\}$  (in which, here and subsequently for other quantities having one term in the parentheses, the term indicates the time instant at which the quantity is evaluated or assumed to arise) of the continuous composite beam. The revised force vector,  $\{M^i(t_1)\}$  ( $\{M^i(t_1)\}^T = \{M_A^i(t_1), M_B^i(t_1)\}$ ) and the revised displacement vector of continuous beam,  $\{D^*(t_1)\}$  ( $\{D^*(t_1)\}^T = \{\theta_A^{i,*}(t_1), \theta_B^{i,*}(t_1)\}$ ) are obtained by adding the force vector and displacement vectors of this analysis to the force vector and displacement vector at the end of previous cycle. The superscript, \* indicates that the end rotations are based on the displacement analysis.

Based on the revised force vector,  $\{M^i(t_1)\}$ , the revised crack lengths of beam elements,  $x_A(t_1)$ ,  $x_B(t_1)$  are established by locating the section at which the tensile stress in the top fiber,  $\sigma_{un}^i(t_1)$  is equal to the tensile strength of concrete,  $f_i(t_1)$ . For the beam element shown in Fig. 8, the stress  $\sigma_{un}^i(t_1)$  for a cross-section at distance  $x$  from end A is obtained from Eqs. (2) and (3), on substitution of  $M^i(t_1)$  by  $R_A^i(t_1)x - M_A^i(t_1) - wx^2/2$ , as

$$\sigma_{un}^i(t_1) = a(t_1)x^2 + b(t_1)x + c(t_1) \quad (38)$$

where  $a(t_1) = -0.5p(t_1)wE_c(t_1)$ ;  $b(t_1) = p(t_1)\Delta R_A^i(t_1)E_c(t_1)$ ;  $c(t_1) = -p(t_1)\Delta M_A^i(t_1)E_c(t_1)$  in which  $p(t_1) = B/(E_c(t_1)(AI - B^2))$ .

The crack lengths  $x_A(t_1)$ ,  $x_B(t_1)$  can now be expressed in the closed form, on equating  $\sigma_{un}^i(t_1)$  with  $f_i(t_1)$ , as

$$x_A(t_1) = \frac{-b(t_1) + \sqrt{[b(t_1)]^2 - 4a(t_1)[c(t_1) - f_i(t_1)]}}{2a(t_1)} \quad (39)$$

$$x_B(t_1) = L + \frac{b(t_1) + \sqrt{[b(t_1)]^2 - 4a(t_1)[c(t_1) - f_i(t_1)]}}{2a(t_1)} \quad (40)$$

The interpolation coefficients  $\xi_A(t_1)$ ,  $\xi_B(t_1)$  are evaluated from Eq. (15) on replacing  $f_i$  and by  $f_i(t_1)$  and  $\sigma_{un}$  by  $\sigma_{A,un}(t_1)$ ,  $\sigma_{B,un}(t_1)$  respectively which can be expressed in the closed form as

$$\sigma_{A,un}(t_1) = \frac{a(t_1)(x_A(t_1))^2}{3} + \frac{b(t_1)x_A(t_1)}{2} + c(t_1); \tag{41}$$

$$\sigma_{B,un}(t_1) = \frac{a(t_1)(L^3 - (y_B(t_1))^3)}{3x_B(t_1)} + \frac{b(t_1)(L^2 - (y_B(t_1))^2)}{2x_B(t_1)} + c(t_1) \tag{42}$$

Changes in crack lengths and end rotations lead to the difference between the displacement vector,  $\{D^*(t_1)\}$  obtained from the displacement analysis and the displacement vector,  $\{D(t_1)\}$  ( $\{D(t_1)\}^T = \{\theta_A^{ii}(t_1), \theta_B^{ii}(t_1)\}$ ) obtained by the integrating the curvature diagram with  $m_1$  and  $m_2$  diagrams (see Eqs. (26) and (27) ). This difference or error in displacement vector,  $\{e_d(t_1)\}$  ( $=\{D(t_1)\}-\{D^*(t_1)\}$ ) leads to the residual force vector,  $\{e_f(t_1)\}$  ( $=[k(t_1)] \cdot \{e_d(t_1)\}$ ), where  $[k(t_1)]$  can be evaluated from Eqs. (21)-(23).

The residual force vector of the members,  $\{e_f(t_1)\}$  are assembled to form the residual force vector,  $\{E_f(t_1)\}$  of the continuous composite beam.  $\{E_f(t_1)\}$  should be within some permissible limit (Ghali *et al.* 2002) for the iterative process to terminate, typically  $\{E_f(t_1)\}^T \{E_f(t_1)\} \leq 0.001 \{M_F^0(t_1)\}^T \{M_F^0(t_1)\}$ , where  $\{M_F^0(t_1)\}$  = fixed end force vector for first iteration (zero crack length). Otherwise a new cycle is started.

#### 4.2 Time-dependent analysis

The progressive nature of cracking in beams with time is shown in Fig. 9. This results in change in creep and shrinkage characteristics of beams with time. In order to account for these changes with time, the time-dependent analysis is carried out by dividing the time into a number of time intervals. In a time interval, the crack length is assumed to be constant and equal to that at the beginning of the time interval (Fig. 9). The change in instantaneous bending moment,  $\Delta M^{ii}$  (resulting from the change in crack length) and  $\Delta M^{id}$  are assumed to arise at the specified instants of time  $t_1, t_2, \dots, t_j$  (Fig. 10). In order to have common notation for the instantaneous analysis and the time-dependent analysis,  $M^{ii}(t_1)$  is

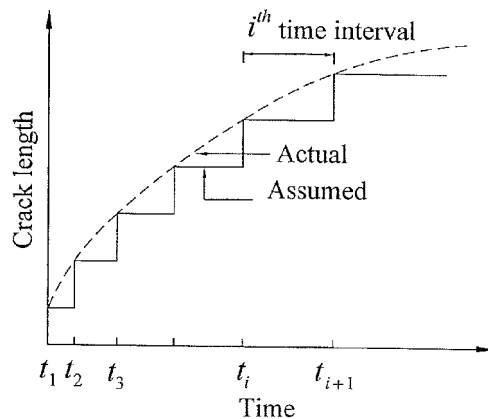


Fig. 9 Progressive nature of cracking

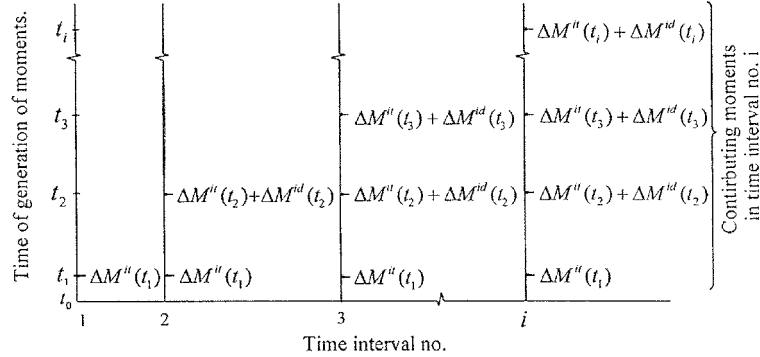


Fig. 10 Time history of generation of moments and contributing moments in a time interval

redesignated as  $\Delta M^u(t_1)$  and the instantaneous curvature, instantaneous top fiber strain, instantaneous top fiber stress at time  $t_1$  are designated as  $\Delta \rho^u(t_1)$ ,  $\Delta \varepsilon^u(t_1)$ ,  $\Delta \sigma^u(t_1)$  respectively.

The displacement method has been used for the time-dependent analysis also in which the fixed end forces owing to creep and shrinkage and stiffness matrix of a beam element for a time interval are required.

Consider the first time interval  $(t_1, t_2)$ . For the evaluation of the fixed end forces and the stiffness matrix, the cracked span length released beam element is considered. Owing to the creep in the cross-section of uncracked zone and uncracked state of the cracked zone, the curvature  $\Delta \rho_{un}^u(t_1)$  changes by a factor  $\Delta \beta_{un}^c(t_2, t_1, t_1)$  (see Eq. (8)), leading to the change in curvature  $\Delta \rho_{un}^c(t_2, t_1, t_1)$  ( $= \Delta \rho_{un}^u(t_1) \Delta \beta_{un}^c(t_2, t_1, t_1)$ ) in which, here and subsequently for other quantities having three terms in the parentheses, the first and second terms indicate the time of the end and the beginning of the interval (for which the change in a quantity is evaluated) respectively and the third term indicates the time of initiation of a cause from which the change arises. The cause may be either application of a moment or the shrinkage. Presently the quantity is the curvature and cause is the application of the moment  $\Delta M^u(t_1)$ . The factor  $\Delta \beta_{un}^c(t_2, t_1, t_1)$  is given as  $\Delta \beta_{un}^c(t_2, t_1) - \Delta \beta_{un}^c(t_1, t_1)$  in which, here and subsequently for other quantities having two terms in the parentheses, the first term indicates the time instant at which a quantity is evaluated whereas the second term indicates the time of initiation of the cause owing to which the quantity arises. The cause may be either application of the moment or shrinkage or gradual application of unit load (required for evaluation of age-adjusted flexibility matrix and hence stiffness matrix) or application of stress (required for evaluating  $\bar{E}_e$ ). The factor  $\Delta \beta_{un}^c(t_2, t_1)$  is evaluated from Eq. (8) in which  $\Delta \phi$  is replaced by  $\Delta \phi(t_2, t_1)$  and the age-adjusted cross-sectional properties are evaluated using the modular ratio  $E_s / \bar{E}_e(t_2, t_1)$ . In turn,  $\bar{E}_e(t_2, t_1)$  is evaluated using  $\Delta \phi(t_2, t_1)$  and  $\chi(t_2, t_1)$ . It may be noted that  $\Delta \beta_{un}^c(t_1, t_1) = 0$ . As stated earlier, in the cracked zone there is no change in curvature of the cross-section in the cracked state. The changes in the rotations of the released beam element at end A,  $\Delta \theta_A^c(t_2, t_1, t_1)$  and at end B,  $\Delta \theta_B^c(t_2, t_1, t_1)$  resulting from  $\Delta \rho_{un}^c(t_2, t_1, t_1)$  are evaluated from Eqs. (30) and (31) respectively in which  $\Delta \beta_{un}^c$  is replaced by  $\Delta \beta_{un}^c(t_2, t_1, t_1)$ .

Shrinkage is assumed to start from time  $t_1$ , the time of application of first load. Owing to the shrinkage, the change in curvature,  $\Delta \rho_{un}^s(t_2, t_1, t_1)$  of a cross-section of uncracked zone and the uncracked state of the cracked zone is given as  $\Delta \rho_{un}^s(t_2, t_1) - \Delta \rho_{un}^s(t_1, t_1)$ . The quantity  $\Delta \rho_{un}^s(t_2, t_1)$  is evaluated from Eq. (9) on replacing  $\Delta \varepsilon^{sh}$  by  $\Delta \varepsilon^{sh}(t_2, t_1)$  and the age-adjusted properties are used in a manner similar to that described earlier for  $\Delta \beta_{un}^c(t_2, t_1)$ . Here again, it may be noted that  $\Delta \rho_{un}^s(t_1, t_1) = 0$  and also that, in the cracked zone there is no change in curvature of the cross-section

in the cracked state. Changes in the end rotations of the released beam  $\Delta\theta_A^s(t_2, t_1, t_1)$ ,  $\Delta\theta_B^s(t_2, t_1, t_1)$  resulting from  $\Delta\rho_{un}^s(t_2, t_1, t_1)$  are evaluated from Eqs. (33) and (34) respectively in which  $\Delta\rho_{un}^s$  is replaced by  $\Delta\rho_{un}^s(t_2, t_1, t_1)$ .

The total change in end rotations of the released beam element,  $\Delta\theta_A^{cs}(t_3, t_2, t'')$  and  $\Delta\theta_B^{cs}(t_3, t_2, t'')$ , due to creep and shrinkage in the first time interval are now given as

$$\Delta\theta_A^{cs}(t_2, t_1, t'') = \Delta\theta_A^c(t_2, t_1, t_1) + \Delta\theta_A^s(t_2, t_1, t_1) \quad (43)$$

$$\Delta\theta_B^{cs}(t_2, t_1, t'') = \Delta\theta_B^c(t_2, t_1, t_1) + \Delta\theta_B^s(t_2, t_1, t_1) \quad (44)$$

where the Prime on the third term in the parentheses of the quantities  $\Delta\theta_A^{cs}$ ,  $\Delta\theta_B^{cs}$  and in other quantities mentioned subsequently indicates more than one cause, the time of initiation of which are indicated by the third term in the parentheses of the quantities on the right hand side of the equations. Presently the causes are: (1) creep due to moment,  $\Delta M^i(t_1)$  applied at time  $t_1$  and (2) shrinkage beginning from time  $t_1$ .

The vector of fixed end forces,  $\{M_F^{cs}(t_2, t_1, t'')\}$  required to restrain these changes in end rotations are given as  $[\bar{k}_e(t_2, t_1)] \{d^{cs}(t_2, t_1)\}$  where  $\{d^{cs}(t_2, t_1)\}^T = \{\Delta\theta_A^{cs}(t_2, t_1, t''), \Delta\theta_B^{cs}(t_2, t_1, t'')\}$  and the age-adjusted stiffness terms  $\bar{k}_{e,11}, \bar{k}_{e,12}, \bar{k}_{e,21}, \bar{k}_{e,22}$  are evaluated from Eqs. (21) - (23) on replacing  $E_c J_{un}^{na}$  by  $\bar{E}_e J_{e,un}^{na}$ .

These vectors of fixed end forces of beam elements are assembled and a displacement analysis is carried out using the age-adjusted stiffness matrices. This displacement analysis leads to the moment,  $\Delta M^{id}(t_2)$  at a section. The total bending moment,  $M^i(t_2)$  at a cross-section of a beam element at the end of first time interval is given as  $M^i(t_2) = \Delta M^i(t_1) + \Delta M^{id}(t_2)$ .

The deflection at mid-span of a beam element,  $d_m^i(t_2)$  at the end of the first time interval is obtained from Eq. (37), as

$$d_m^i(t_2) = \Delta d_m^i(t_1) + \Delta d_m^c(t_2, t_1, t_1) + \Delta d_m^s(t_2, t_1, t_1) + \Delta d_m^{id}(t_2) \quad (45)$$

where  $\Delta d_m^i(t_1)(= d_m^i)$ ,  $\Delta d_m^c(t_2, t_1, t_1)(= \Delta d_m^c)$ ,  $\Delta d_m^s(t_2, t_1, t_1)(= \Delta d_m^s)$  and  $\Delta d_m^{id}(t_2)(= \Delta d_m^{id})$  are obtained from Eqs. (29), (32), (35) and (36) respectively on replacing  $E_c, \bar{E}_e, M_A^i, M_B^i, R_A^i, R_B^i, \Delta M_A^i, \Delta M_B^i, x_A, x_B, \xi_A, \xi_B$  by  $E_c(t_1), \bar{E}_e(t_2, t_1), \Delta M_A^i(t_1), \Delta M_B^i(t_1), \Delta R_A^i(t_1), \Delta R_B^i(t_1), \Delta M_A^i \Delta R_A^i(t_2), \Delta M_B^i \Delta R_B^i(t_2), \Delta R_A^i(t_2), x_A(t_1), x_B(t_1), \xi_A(t_1), \xi_B(t_1)$  respectively and  $\Delta\beta_{un}^c, \Delta\rho_{un}^s$  by  $\Delta\beta_{un}^c(t_2, t_1, t_1), \Delta\rho_{un}^s(t_2, t_1, t_1)$  respectively.

The revised crack lengths are established by locating the cross-section, at which the tensile stress in the top fiber,  $\sigma_{un}^i(t_2)$  is equal to the tensile strength of concrete,  $f_t(t_2)$ , as is done for instantaneous analysis. First the stress  $\sigma_{un}^i(t_2)$  is expressed in the same form as Eq. (38). On using Eq. (10) for evaluation of and  $\Delta\varepsilon_{un}^c(t_2, t_1)(= \Delta\varepsilon_{un}^i(t_1) \Delta\lambda_{un}^c(t_2, t_1))$  and  $\Delta\varepsilon_{un}^s(t_1, t_1)(= \Delta\varepsilon_{un}^i(t_1) \Delta\lambda_{un}^s(t_1, t_1))$ , the stress  $\sigma_{un}^i(t_2)$ , may be expressed from Eq. (14) as

$$\begin{aligned} \sigma_{un}^i(t_2) = & \Delta\sigma_{un}^i(t_1) + \bar{E}_e(t_2, t_1) [\Delta\varepsilon_{un}^i(t_2, t_1) [\Delta\lambda_{un}^c(t_2, t_1) - \Delta\phi(t_2, t_1)] + \Delta\varepsilon_{un}^s(t_2, t_1) - \Delta\varepsilon^{sh}(t_2, t_1)] \\ & - \bar{E}_e(t_1, t_1) [\Delta\varepsilon_{un}^i(t_1, t_1) [\Delta\lambda_{un}^c(t_1, t_1) - \Delta\phi(t_1, t_1)] + \Delta\varepsilon_{un}^s(t_1, t_1) - \Delta\varepsilon^{sh}(t_1, t_1)] + \Delta\sigma_{un}^{id}(t_2) \end{aligned} \quad (46)$$

Further, on using Eq. (2) for evaluation of  $\Delta\varepsilon_{un}^i(t_1)$ , Eq. (11) for evaluation of  $\Delta\varepsilon_{un}^s(t_2, t_1)$  and  $\Delta\varepsilon_{un}^s(t_1, t_1)$ ,

and rearranging the terms, Eq. (46) may be expressed in the same form as Eq. (38):

$$\sigma_{un}^i(t_2) = a(t_2)x^2 + b(t_2)x + c(t_2) \quad (47)$$

where  $a(t_2)$ ,  $b(t_2)$ ,  $c(t_2)$  are given in Appendix B

Since Eq. (47) is of the same form as Eq. (38), the crack lengths  $x_A(t_2)$ ,  $x_B(t_2)$  and the representative stress,  $\sigma_{A,un}(t_2)$ ,  $\sigma_{B,un}(t_2)$  are obtained from Eqs. (39)- (42) respectively on replacing the terms in the parentheses  $t_1$  by  $t_2$ .

Now consider the second time interval ( $t_2, t_3$ ). In addition to the two forces,  $\Delta M^{id}(t_1)$  generated at time  $t_1$  and  $\Delta M^{id}(t_2)$  generated at time  $t_2$ , a force  $\Delta M^{ii}(t_2)$  that results from change in crack lengths in the previous time interval ( $t_1, t_2$ ) needs to be considered in this time interval ( $t_2, t_3$ ). Thus creep in this interval is caused due to one force ( $\Delta M^{ii}(t_1)$ ) generated at time  $t_1$  and two forces ( $\Delta M^{ii}(t_2)$ ,  $\Delta M^{id}(t_2)$ ) generated at time  $t_2$  (Fig. 10). The bending moment,  $\Delta M^{ii}(t_2)$  is obtained by carrying out a displacement analysis for which the fixed end force vector is taken equal to the change in fixed end forces owing to change in the crack lengths.

Further analysis proceeds in the similar manner as explained for the first time interval. In the  $i$ th time interval ( $t_i, t_{i+1}$ ), there are  $1+2(i-1)$  number of forces causing creep as shown in Fig. 10. The creep effect of  $1+2(i-1)$  number of forces and the shrinkage effect can be evaluated in a similar manner as explained for the first time interval. The total deflection and the stress at the top fiber of a cross-section can be expressed in a form similar to that of Eq. (45) and (47) respectively. The number of time intervals is decided on the criteria that the change in the values of moments,  $M$  and mid-span deflections,  $d_m$  for any span, with increase in number of time intervals, should not be more than 1%.

## 5. Validation and numerical study

In order to validate the proposed procedure, first, the results have been compared with the experimental results reported by Gilbert and Bradford 1992 for two two-span continuous composite beams B1, B2 of length  $L_1 = L_2 = 5.8$  m [Fig. 11(a)]. The relevant cross-sectional properties of the beams are shown in the Fig. 12 and Table 1. The beam B1 was subjected to a superimposed uniformly distributed span load ( $w$ ) of 4.45 kN/m in addition to the dead load (1.92 kN/m) whereas beam B2 was subjected to dead load only. The beams were tested for a period of 340 days and the mid-span

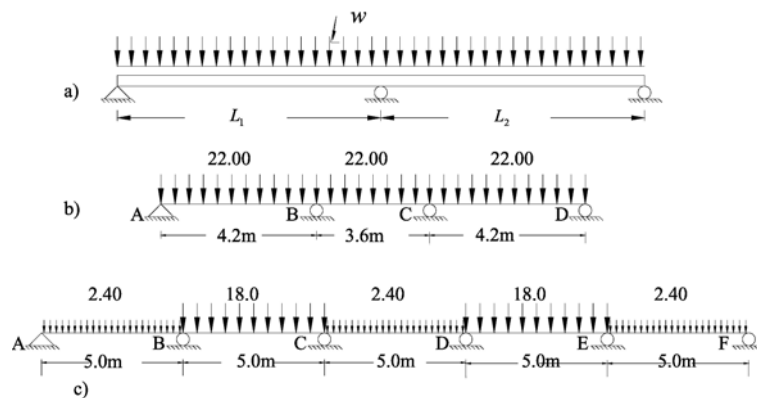


Fig. 11 Longitudinal profile of (a) beams B1, B2, B3, B4; (b) beam B5; and (c) beam B6 (load case 1)

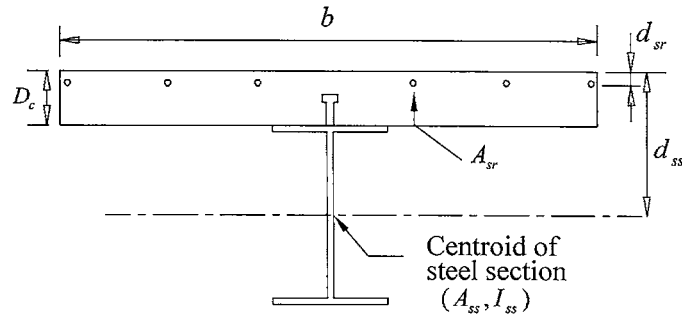


Fig. 12 Cross-section of beams B1, B2, B3, B4, B5 and B6

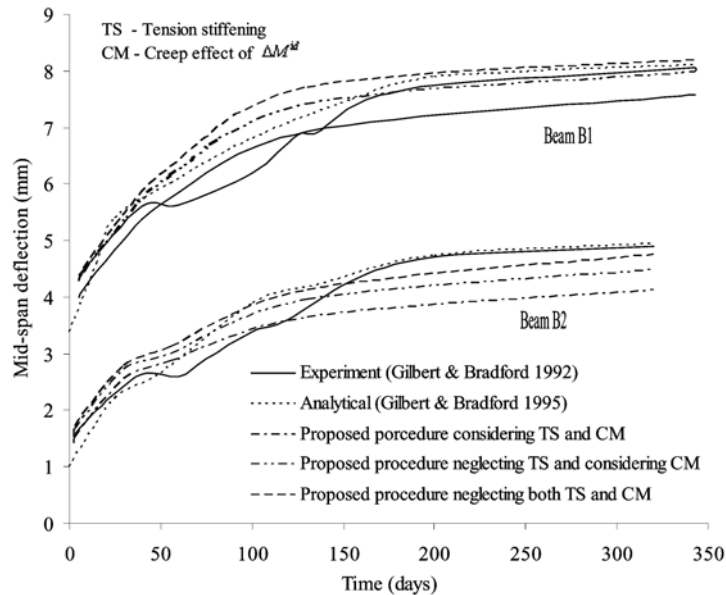


Fig. 13 Comparison of mid-span deflections of beams B1 and B2

deflections of beams were measured during the test.

The mid-span deflections obtained by the proposed procedure have been compared with the mid-span deflections reported by the above experimental study and also with the analytical results of Gilbert and Bradford (1995). The values obtained from the proposed procedure considering tension stiffening (TS) and creep effect of  $\Delta M^{id}$  (CM) are in reasonable agreement with the reported experimental values of mid-span deflections (Fig. 13). The values of mid-span deflections obtained from the proposed procedure for both the beams are lower than the analytical values reported by Gilbert and Bradford 1995. The higher values of analytical procedure can be ascribed to: (1) neglect of TS, (2) neglect of CM and (3) the manner in which the crack length is established i.e., same crack length is assumed for the entire time interval which begins from the time of application of load. Therefore two more sets of results were obtained from the proposed procedure: (1) neglecting TS and considering CM and (2) neglecting both TS and CM. These deflections are also shown in Fig. 13. As expected, the values obtained from the proposed procedure now are closer to the analytical results.

In order to study the effect of tension stiffening further, the instantaneous and long-term mid-span

Table 1 Cross-sectional properties of beams considered for validation and numerical study

Beam	$b$ (mm)	$D_c$ (mm)	$D_s$ (mm)	$d_{sr}$ (mm)	$A_{ss}$ (mm <sup>2</sup> )	$A_{sr}$ (mm <sup>2</sup> )	$I_{ss}$ (mm <sup>4</sup> )	$f_t$ (N/mm <sup>2</sup> )	$E_c$ (N/mm <sup>2</sup> )	$E_s$ (N/mm <sup>2</sup> )	$\Delta\phi$	$\Delta\varepsilon^{sh}$
B1,B2	1000	70	203	15.0	3230	113	$23.6 \times 10^6$	-3.0	22000	$2 \times 10^5$	1.68	0.00052
B3,B4	1000	100	254	15.0	3620	113	$40.04 \times 10^6$	-3.0	25000	$2 \times 10^5$	2.00	0.0003
B5	1000	75	254	15.0	3210	254	$34.04 \times 10^6$	-3.0	22600	$2 \times 10^5$	1.74	0.0003
B6	1000	75	254	15.0	3210	254	$34.04 \times 10^6$	-3.0	22600	$2 \times 10^5$	1.74	0.0003

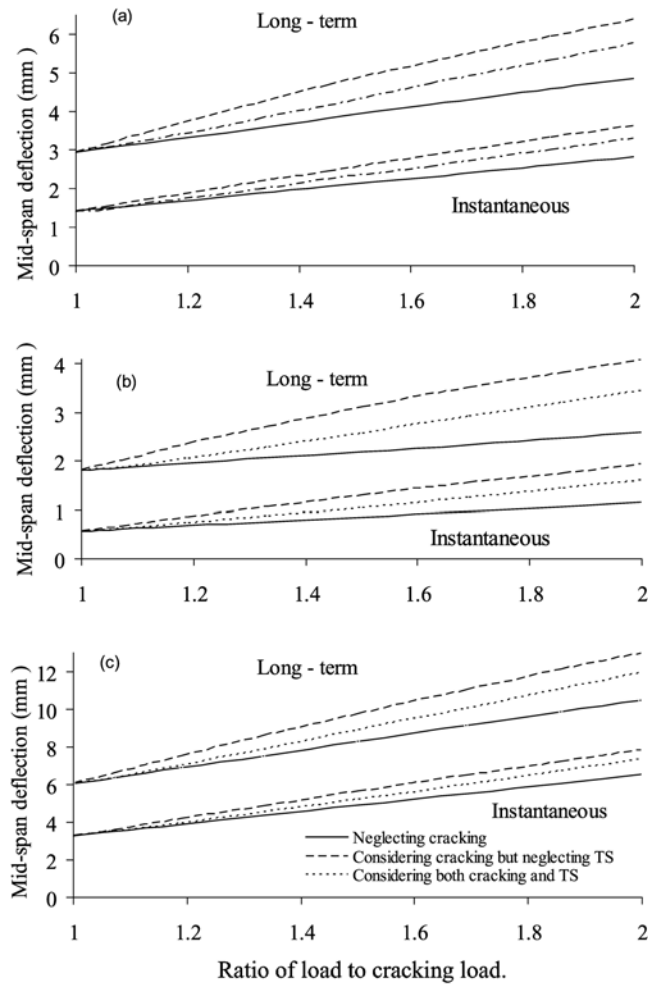


Fig. 14 Effect of cracking and tension stiffening on mid-span deflections of (a) beam B3; (b) shorter span of beam B4; (c) larger span of beam B4

deflections have been obtained for other two-span continuous composite beams of different span and span ratio [Figs. 11(a) and 12]. These beams are designated as B3 and B4. Beam B3 is symmetrical with span lengths  $L_1 = L_2 = 6.0$  m, whereas beam B4 is unsymmetrical with span lengths  $L_1 = 6.0$  m;  $L_2 = 7.5$  m. The cross-sectional properties of both the beams are the same and given in Table 1. Mid-

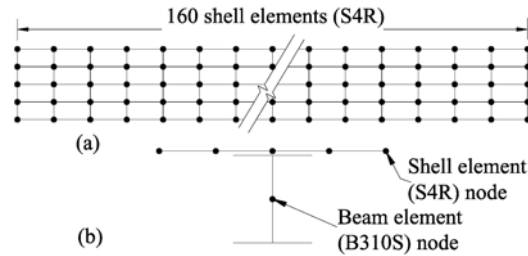


Fig. 15 Finite element mesh of entire composite beam B5: (a) shell elements in slab; and (b) nodes in the cross-section

span deflections of the beams are obtained from the proposed procedure for three cases: (1) neglecting cracking, (2) considering cracking but neglecting TS and (3) considering both cracking as well as TS. The beams have been subjected to a loading range, which varies from the cracking load (the load at which the first crack occurs at the mid-support at the time of application of load) to twice the cracking load. These deflections are shown in Figs. 14(a) to 14(c). It can be observed from these figures that there is a considerable effect of tension stiffening on both the instantaneous as well as long-term mid-span deflections of the beams. The effect increases with the increase in loading on the beam. For the example considered, the maximum effect is up to 23.1% for the shorter span in unsymmetrical beam.

Next, the results obtained from the proposed procedure have been validated by comparison with those obtained from ABAQUS (a finite element software), for a three span beam designated as beam B5 [see Figs. 11(b), 12 and Table 1]. Two types of meshes, fine and coarse have been considered. The fine mesh (Fig. 15) for the entire composite beam consists of 160(40×4) shell elements (S4R elements) and 40 beam elements (B310S elements) whereas the coarse mesh consists of 40(20×2) S4R elements and 20 B310S elements. The condition of no slip between the slab and the steel section is achieved by using multipoint constraints (MPC'S), of type BEAM, between corresponding shell and beam elements. Creep of the concrete is taken into account by modeling concrete as viscoelastic material in time domain whereas shrinkage is taken into account by applying equivalent temperature loading (temperature and coefficient of thermal expansion are assumed to vary in such a manner that the thermal strain of concrete at any instant of time is equal to  $\Delta\epsilon^{sh}$ ). Considering the fact that the viscoelastic material model cannot be combined with the cracking in ABAQUS, two type of analyses have been considered: (1) instantaneous analysis considering cracking, (2) time-dependent analysis neglecting cracking. For each analysis,  $w = 22 \text{ kN/m}$  is considered.

First, consider analysis 1.  $w$  is assumed to be applied at 3 days. The values of bending moment,  $M_{BC}$  and  $d_m$  of beam AB using fine and coarse meshes are found to be 38.14 kN-m, 38.26 kN-m respectively and 2.91 mm, 2.87 mm respectively. Therefore, the fine mesh is adequate and is considered for validation. The values of  $M_{BC}$  and  $d_m$  obtained from the proposed procedure for analysis 1 are 38.27 kN-m and 2.68 mm respectively. The percentage differences in  $M_{BC}$  and  $d_m$  are 0.33% and 8.02% respectively. Now consider analysis 2.  $w$  is assumed to be applied at 28 days. The values of bending moment,  $M_{BC}$  and  $d_m$  for span AB obtained from ABAQUS and proposed procedure are 54.29 kN-m, 51.66 kN-m respectively and 4.31 mm and 3.92 mm respectively. The percentage differences in  $M_{BC}$  and  $d_m$  are 4.44% and 9.05% respectively. Therefore, for both the analyses, the results obtained from the proposed procedure (PP) are in reasonable agreement with the results obtained from ABAQUS. Major portions of the differences between the results may be due to the consideration of biaxial state of stress in ABAQUS and due to introduction of MPC's (type BEAM) between only one node each of

Table 2 Results of numerical studies for beam B6

Load Case	Analysis Type	Moment (kN-m)		*Deflection $d_m$ (mm)		
		$M_{BC}$	$M_{CB}$	Span AB	Span BC	Span CD
1	Instantaneous	26.58	20.18	-1.13	3.77	-2.23
	Time-dependent	41.59	31.53	-0.59	4.74	-2.84
2	Instantaneous	26.50	20.19	5.40	-2.75	4.28
	Time-dependent	41.47	31.54	8.06	-3.89	5.79
3	Instantaneous	22.25	38.34	-0.78	2.64	1.32
	Time-dependent	37.45	49.25	-0.15	3.27	1.96

\*positive value: downward deflection

adjacent shell elements and a beam element (only available nodes for the connection in the chosen finite element model) across a cross-section. Further, in analysis 2, some difference would also result from choice of the same value of  $\chi$  for creep and shrinkage. However, this difference is likely to be small.

It may be noted that the total number of degrees of freedom for the composite beams in the proposed procedure is 12 whereas the corresponding number of degrees of freedom for ABAQUS is 1517. Therefore, the computational effort required for the proposed procedure is a small fraction of that required for the finite element analysis.

Further numerical studies have been carried out for a five span beam (Beam B6). The cross-sectional properties of the beam are listed in Table 1. The beam is subjected to different load cases. In each case some spans are assumed to be subjected to only self weight,  $w_d = 2.4$  kN/m and other spans are assumed to be subjected to self weight, superimposed dead load and live load,  $w_l = 18$  kN/m. The load case 1 is shown in Fig.11(c) where spans AB, CD, EF are subjected to  $w_d$ , whereas spans BC and DE are subjected to  $w_l$ . In load case 2, spans BC and DE are subjected to  $w_d$ , whereas spans AB, CD and EF are subjected to  $w_l$ . In load case 3, spans AB and EF are subjected to  $w_d$ , whereas spans BC, CD and DE are subjected to  $w_l$ . Taking into account the symmetry of the beam, moments  $M_{BC}$  and  $M_{CB}$  along with mid-span deflection,  $d_m$  of spans AB, BC and CD have been presented in Table 2. It is observed from the results that, due to time-dependent effects of creep and shrinkage, the increase in moment,  $M_{BC}$  is up to 68.31% (load case 3) whereas  $M_{CB}$  increases by up to 18.88% (load case 1). The increase in positive mid-span deflection is up to 48.16% (for span AB in load case 2). Therefore, there is a considerable redistribution of moments and change in deflections due to creep and shrinkage.

## 6. Conclusions

An analytical-numerical procedure has been presented in this paper to take into account the non-linear effects of concrete cracking and time-dependent effects of creep and shrinkage in the concrete portion of the continuous composite beams under service load. The procedure is analytical at the element level and numerical at the structural level. Closed form expressions for stiffness matrix, load vector, crack lengths and mid-span deflection of the cracked span length beam element have been presented. The results obtained from the proposed procedure are shown to be in reasonable agreement with the experimental, analytical and finite element results. It is concluded from the numerical study carried out that the effect of tension stiffening on mid-span deflection of composite beams can be significant. The proposed procedure can be readily extended for the analysis of composite building

frames where saving in computational effort would be very considerable.

## References

- Amadio, C. and Fragiaco, M. (1997), "A simplified approach to evaluate creep and shrinkage effects in steel concrete composite beams", *J. Struct. Eng.*, ASCE, **123**(9), 1153-1162.
- Albrecht, G., Kurita A., Rutner M. and Ohyama, O. (2003), "The long term tension stiffening at composite bridge construction", 5<sup>th</sup> *Japanese-German Joint Symposium on Steel and Composite Bridges*. Osaka, Sept.
- Bradford, M. A. and Gilbert, R. I. (1991), "Experiments on composite tee-beams at service loads", *Civ. Eng. Trans.*, IE Aust, Australia, CE **33**(4), 285-291.
- Bradford, M. A. and Gilbert, R. I. (1992), "Composite beams with partial interaction under service loads", *J. Struct. Eng.*, ASCE, **118**(7), 1871-1883.
- Bradford, M. A., Manh, H. Vu. and Gilbert R. I. (2002), "Numerical analysis of continuous composite beams at service loading", *Adv Struct. Eng.*, **5**(1), 1-12.
- CEB-FIP (1990), "*Model Code for Concrete Structures*", CEB, Thomas Telford, London.
- Dezi, L. and Tarantino, A. M. (1993a), "Creep in composite continuous beams: I: Theoretical treatment", *J. Struct. Eng.*, ASCE, **119**(7), 2095-2111.
- Dezi, L. and Tarantino, A. M. (1993b), "Creep in composite continuous beams. II: Parametric Study", *J. Struct. Eng.*, ASCE, **119**(7), 2112-2133.
- Dezi, L., Leoni, G. and Tarantino, A. M. (1995), "Time dependent analysis of prestressed composite beams", *J. Struct. Eng.*, ASCE, **121**(4), 621-633.
- Dezi, L., Leoni, G. and Tarantino, A. M. (1996), "Algebraic method for creep analysis of continuous composite beams", *J. Struct. Eng.*, ASCE, **122**(4), 423-430.
- Elbadry, M., Youakim, S. and Ghali, A. (2003), "Model analysis of time-dependent stresses and deformations in structural concrete", *Prog. Struct. Eng. Mater.*, **5**, 153-166.
- Frangiaco, M., Amadio, C. and Macorini, L. (2004), "Finite element model for collapse and long-term analysis of steel-concrete composite beams", *J. Struct. Eng.*, ASCE, **130**(3), 489-497.
- Ghali, A., Favre, R. and Elbadry, M. (2002), "*Concrete Structures: Stresses and Deformations*", Third Edition, Spon Press, London.
- Gilbert, R. I. (1988), *Time effects in concrete structures*, Elsevier, Amsterdam, The Netherlands.
- Gilbert, R. I. and Bradford, M. A. (1992), "Time-dependent behavior of continuous composite beams at service loads", *UNICIV Rep.R-307*, School of Civil Eng., Univ. of New South Wales, Sydney, Australia.
- Gilbert, R. I. and Bradford, M. A. (1995), "Time-dependent behavior of composite beams at service loads", *J. Struct. Eng.*, ASCE, **121**(2), 319-327.
- Kwak, G. H. and Seo, Y. G. (2000), "Long term behavior of composite girder bridges", *Comput. Struct.*, **74**(5), 583-599.
- Kwak, G. H. and Seo, Y. G. (2002a), "Shrinkage cracking at interior supports of continuous precast prestressed concrete girder bridges", *Const. and Bldg. Mater.*, **16**, 35-47.
- Kwak, G. H. and Seo, Y. G. (2002b), "Numerical analysis of time-dependent behavior of pre-cast pre-stressed concrete girder bridges", *Const. and Bldg. Mater.*, **16**, 49-63.
- Mari, A., Mirambell, E. and Estrada, I. (2003), "Effect of construction process and slab prestressing on the serviceability behavior of composite bridges", *J. Const. Steel Res.*, **59**, 135-163.
- Sakr, M. and Lapos, J. (1998), "Time-dependent analysis of partially prestressed continuous composite beams", *2nd Int. PhD Symposium in Civil Eng.*, Budapest.

## Notation

- $A, B, I$  : area, first moment of area and second moment of area of transformed section about reference axis, respectively
- $A_c, B_c, I_c$  : area, first moment of area and second moment of area of concrete about reference axis, respectively

$\bar{A}_e, \bar{B}_e, \bar{I}_e$	: age-adjusted transformed area, first moment of area and second moment of area about reference axis, respectively
$b, D_c$	: width and depth of concrete
$A_{sr}, d_{sr}$	: area of reinforcement in slab and its depth from top fiber, respectively
$A_{ss}, I_{ss}, D_s$	: area, moment of inertia and depth of steel section, respectively
$\{D^*(t_1)\}, \{D(t_1)\}$	: displacement vectors of continuous beam during an iterative cycle at time $t_1$
$d_m^i, d_m^{it}, \Delta d_m^i, \Delta d_m^{it}, \Delta d_m^{id}$	: mid-span deflections
$E_c, E_s$	: modulus of elasticity of concrete and steel, respectively
$\bar{E}_e(t_i, t_j)$	: age-adjusted effective modulus of concrete at time $t_i$ for loading at time $t_j$
$\{d^{cs}(t_{i+1}, t_i)\}$	: displacement vector for $i$ th time interval
$\{e_d(t_1)\}$	: error in displacement vector of beam element, during an iterative cycle at time $t_1$
$\{e_F(t_j)\}, (E_F(t_j))$	: residual force vector of a beam element and continuous beam respectively, during an iterative cycle at time $t_1$
$f(t_j)$	: tensile strength of concrete at time
$f_{11}, f_{12}, f_{21}, f_{22}$	: flexibility coefficients
$I_{um}^{na}, I_{cr}^{na}$	: moment of inertia of cross-section about neutral axis
$I_e^{na}, I_{um}^{na}$	: age-adjusted moment of inertia about neutral axis
$k_{11}, k_{12}, k_{21}, k_{22}$	: stiffness coefficients
$[k(t_j)]$	: stiffness matrix at time $t_j$
$[\bar{k}_e(t_{i+1}, t_i)]$	: age-adjusted stiffness matrix for $i$ th time interval
$L, L_1, L_2$	: span lengths
$m_1, m_2$	: moment at a section due to unit end moments
$\{M^i(t_j)\}$	: force vector during an iterative cycle at time $t_1$
$\{M_F^e(t_2, t_1, t'')\}$	: vector of fixed end moments required to restrain the rotations owing to creep and shrinkage in $i$ th time interval
$\{M_F^0(t_1)\}$	: fixed end force vector in first iterative cycle at time $t_1$
$R_A^i, R_B^i, \Delta R_A^i, \Delta R_B^i, \Delta R_A^{id}, \Delta R_B^{id}$	: shears at ends
$M_A^i, M_B^i, \Delta M_A^i, \Delta M_B^i, \Delta M_A^{id}, \Delta M_B^{id}$	: moments at ends
$x_A(t_j), x_B(t_j)$	: crack lengths at time $t_j$
$y_A(t_j), y_B(t_j)$	: length $L-x_A(t_j)$ and $L-x_B(t_j)$ respectively
$w$	: uniformly distributed span load
$\theta_A^i, \theta_B^i, \theta_A^{i,*}, \theta_B^{i,*}$	: instantaneous end rotations
$\rho_{um}^{it}(t_j), \rho_{cr}^{it}(t_j), \rho_{is}^{it}(t_j), \rho_{um}^l(t_j), \rho_{is}^l(t_j)$	: curvatures at time $t_j$
$\varepsilon_{um}^{it}(t_j), \varepsilon_{cr}^{it}(t_j), \varepsilon_{is}^{it}(t_j), \varepsilon_{um}^l(t_j), \varepsilon_{is}^l(t_j)$	: top fiber strains at time $t_j$
$\sigma_{um}^{it}(t_j), \sigma_{cr}^{it}(t_j), \sigma_{is}^{it}(t_j), \sigma_{um}^l(t_j)$	: top fiber stresses at time $t_j$
$\xi_A(t_j), \xi_B(t_j)$	: interpolation coefficients at time $t_j$
$\phi_u$	: vultimate creep coefficient
$\Delta \phi(t_i, t_j)$	: creep coefficient at time $t_i$ for load applied at time $t_j$
$\Delta \varepsilon^{sh}(t_j, t_1)$	: shrinkage strain at time $t_j$ for shrinkage beginning from time $t_1$
$\chi(t_i, t_j)$	: aging coefficient corresponding to $\Delta \phi(t_i, t_j)$
$\Delta M^i(t_j)$	: change in instantaneous bending moment at time $t_j$
$\Delta M^{id}(t_j)$	: additional moment generated in indeterminate structure at time $t_j$ due to creep and shrinkage
$\Delta \beta_{um}^c$	: factor by which a curvature changes due to creep
$\Delta \beta_{um}^c(t_i, t_j)$	: $\Delta \beta_{um}^c$ at time $t_i$ for loading at time $t_j$
$\Delta \beta_{um}^c(t_{i+1}, t_i, t_j)$	: $\Delta \beta_{um}^c(t_{i+1}, t_j) - \Delta \beta_{um}^c(t_i, t_j)$

$\Delta \rho_{un}^s, \Delta \rho_{un}^{cs}$	: changes in curvature of a cross section
$\Delta \rho^{it}(t_j), \Delta \varepsilon^{it}(t_j), \Delta \sigma^{it}(t_j)$	: curvature, top fiber strain and top fiber stress respectively due to $\Delta M^{it}(t_j)$
$\Delta \rho_{un}^c(t_{i+1}, t_i, t_j), \Delta \rho_{un}^s(t_{i+1}, t_i, t_j)$	: changes in curvature in the $i$ th time interval due to creep effect of a moment applied at time, $t_j$ and beginning of shrinkage at time $t_1$
$\Delta \theta_A^i, \Delta \theta_B^i$	: end rotations due to $\Delta M^{it}$
$\Delta \theta_A^c(t_{i+1}, t_i, t_j), \Delta \theta_B^c(t_{i+1}, t_i, t_j)$	: change in end rotations in $i$ th time interval due to creep effect of moment applied at time $t_j$
$\Delta \theta_A^s(t_{i+1}, t_i, t_j), \Delta \theta_B^s(t_{i+1}, t_i, t_j)$	: change in rotations at ends of released beam element in $i$ th time interval due to shrinkage beginning from time $t_1$
$\Delta \theta_A^{cs}(t_{i+1}, t_i, t_j), \Delta \theta_B^{cs}(t_{i+1}, t_i, t_j)$	: total change in rotation at ends A and B of released beam in the $i$ th time interval due to more than one number of cause
$\Delta \rho_{un}^{id}(t_j), \Delta \rho_{cr}^{id}(t_j), \Delta \rho_{ts}^{id}(t_j)$	: curvatures due to $\Delta M^{id}(t_j)$
$\Delta \varepsilon_{un}^{id}(t_j), \Delta \varepsilon_{cr}^{id}(t_j), \Delta \varepsilon_{ts}^{id}(t_j)$	: top fiber strains at time $t_j$ due to $\Delta M^{id}(t_j)$
$\Delta \sigma_{un}^{id}(t_j)$	: top fiber stress due to $\Delta M^{id}(t_j)$

### Subscript

<i>un</i>	: uncracked cross section or uncracked state
<i>cr</i>	: cracked state
<i>ts</i>	: tension stiffening
<i>A, B</i>	: ends <i>A</i> and <i>B</i> respectively

### Superscript

<i>it</i>	: instantaneous value
<i>id</i>	: indeterminate
<i>t</i>	: total value
<i>c,s</i>	: creep and shrinkage respectively
<i>cs</i>	: both creep and shrinkage
"	: more than one cause
*	: displacement analysis

## Appendix A

The flexibility coefficients  $f_{11}, f_{12}, f_{21}, f_{22}$  are expressed in closed form as

$$f_{11} = [1/(3L^2)][(\xi_B x_B^3 - \xi_A x_A^3)(1/(E_c I_{cr}^{na}) - 1/(E_c I_{un}^{na})) + L^3(\eta_A/(E_c I_{un}^{na}) + \xi_A/(E_c I_{un}^{na}))] \quad (A1)$$

$$f_{12} = f_{21} = [1/(6L^2)][\xi_A x_A^2(2x_A - 3L) + \xi_B x_B^2(2x_B - 3L)][1/(E_c I_{cr}^{na}) - 1/(E_c I_{un}^{na})] - L/(6E_c I_{un}^{na}) \quad (A2)$$

$$f_{22} = [1/(3L^2)][(\xi_A x_A^3 - \xi_B x_B^3)(1/(E_c I_{cr}^{na}) - 1/(E_c I_{un}^{na})) + L^3(\eta_B/(E_c I_{un}^{na}) + \xi_B/(E_c I_{un}^{na}))] \quad (A3)$$

**Appendix B**

The coefficients  $a(t_2)$ ,  $b(t_2)$ ,  $c(t_2)$  are given as

$$a(t_2) = a(t_1) - 0.5p(t_1)wq(t_2, t_1, t_1) \quad (\text{B1})$$

$$b(t_2) = b(t_1) + p(t_1)\Delta R_A^{it}(t_1)q(t_2, t_1, t_1) + \bar{p}_e(t_2, t_1)\Delta R_A^{id}(t_2)\bar{E}_e(t_2, t_1) \quad (\text{B2})$$

$$c(t_2) = c(t_1) - p(t_1)\Delta M_A^{it}(t_1)q(t_2, t_1, t_1) + r(t_2, t_1, t_1) - \bar{p}_e(t_2, t_1)\Delta M_A^{id}(t_2)\bar{E}_e(t_2, t_1) \quad (\text{B3})$$

$$q(t_2, t_1, t_1) = \bar{E}_e(t_2, t_1)[\Delta \lambda_{un}^c(t_2, t_1) - \Delta \phi(t_2, t_1)] - \bar{E}_e(t_1, t_1)[\Delta \lambda_{un}^c(t_1, t_1) - \Delta \phi(t_1, t_1)] \quad (\text{B4})$$

$$r(t_2, t_1, t_1) = \bar{E}_e(t_2, t_1)[\Delta \varepsilon_{un}^s(t_2, t_1) - \Delta \varepsilon^h(t_2, t_1)] - \bar{E}_e(t_1, t_1)[\Delta \varepsilon_{un}^s(t_1, t_1) - \Delta \varepsilon^h(t_1, t_1)] \quad (\text{B5})$$

The quantity  $\bar{p}_e(t_2, t_1)$  is evaluated in the same way as  $p(t_1)$  using age-adjusted cross-sectional properties.

CC